GrAHal-CAPP for axion dark matter search with unprecedented sensitivity in the 1–3 μeV mass range

Pierre Pugnat[1]*, Philippe Camus[2], Ohjoon Kwon[3]*, Rafik Ballou[2],
Cyril Bruyère[2], Heesu Byun[3], Woohyun Chung[3], Thierry Grenet[2],
Pierre Perrier[2], Yannis K. Semertzidis[3,4], Arthur Talarmin[2] and
Jérémy Vessaire[2]

[1]Laboratoire National des Champs Magnétiques Intenses (LNCMI), European Magnetic Field Laboratory
(EMFL), Université Grenoble-Alpes, Centre National de la Recherche Scientifique (CNRS), Grenoble,
France, [2]Institut Néel, Université Grenoble-Alpes, Centre National de la Recherche Scientifique (CNRS),
Grenoble INP, Grenoble, France, [3]Center for Axion and Precision Physics Research (CAPP), Institute for
Basic Science (IBS), Daejeon, Republic of Korea, [4]Department of Physics, Korea Advanced Institute of
Science and Technology (KAIST), Daejeon, Republic of Korea

A collaboration between CNRS-Grenoble and IBS-CAPP Daejeon plans to build a
Sikivie's type haloscope for axion/ALPs dark matter search at the Dine-Fischler-
Srednicki-Zhitnitskii sensitivity for the 300−600 MHz range. It will be based on
the large-bore superconducting "outsert" coil of the Grenoble hybrid magnet,
providing a central magnetic field up to 9 T in an 810-mm warm bore diameter.
This magnet has recently been successfully powered up to 8.5 T, achieving the
first step of the electrical commissioning phase. The design principles of the
cryostat with its double dilution refrigerators to cool below 50 mK, the light Cu RF
cavity of 700-mm diameter, and its tuning rod(s) and the first stages of the
measurement chain are presented. Perspectives for the targeted sensitivity
assuming less than a 2-year integration time are given.

KEYWORDS

axion, ALPS, dark matter, haloscope, large-bore superconducting magnets, RF cavities,
large scale 3 He/4 He dilution refrigerator, cryogenics

1 Introduction

Particle and astroparticle physics beyond the standard model (SM) are not restricted to
the high-energy frontier. Many extensions of the SM, particularly those based on
supergravity or superstrings, predict not only massive particles like weakly interacting
massive particles (WIMPS) but also weakly interacting sub-eV or slim particles (WISPs).
Whereas WIMPS can be searched for at TeV colliders, such as the Large Hadron Collider
(LHC) at CERN, or in underground experiments, the signatures of WISPs are more likely to
be detected in low-energy laboratory experiments. As the first and paradigmatic examples of
WISPs, there is the axion predicted independently by S. Weinberg [1] and F. Wilczek [2]
from the Peccei and Quin [3] symmetry breaking and which remains one of the most
attractive solutions to the strong-CP problem [4, 5]. In addition, a great number of axions or
axion-like particles (ALPs) are naturally present in string theory of which they constitute a
fundamental underlying feature [5, 6]. The interest in axion/ALP search extends beyond
particle physics because such a hypothetical light spin-zero particle is a leading cold dark

matter candidate [7–10] and the only non-supersymmetric one. This is in the context where no supersymmetric signature was observed to date at either the LHC or in underground experiments [11]. Moreover, axion or ALPs might explain several astrophysical puzzles, such as the Universe's transparency to very high energy photons (>100 GeV) [12], the anomalous white dwarf cooling [13], or the gamma ray excesses in galaxy clusters [14].

2 Principle of the experimental set-up

In 1983, Pierre Sikivie demonstrated that if the cold dark matter (CDM) of our galactic halo is composed of "invisible" axions, they can be detected in a terrestrial laboratory from their conversion to monochromatic photons in a microwave cavity permeated by a magnetic field [15]. The signal power to be detected is then simply given by

$$P = g_{A\gamma\gamma}^2 \left(\rho_{halo}/m_A\right) B^2 V\, C\, Q/2, \tag{1}$$

with $\rho_{halo} \approx 450$ (MeV/c^2)/cm^3 the average CDM density, $m_A \approx 10^{-6}$–10^{-3} eV/c^2 the probed axion mass range as main CDM component, $g_{A\gamma\gamma}$ the unknown axion di-photon coupling constant, B^2V the square of the magnetic field multiplied by the volume of the cavity, $C = 0.5$–0.7 the TM$_{010}$ cavity mode form factor, and the quality factor $Q = 10^4$–10^6. The resonant conversion condition is obtained when the frequency of the cavity is equal to the axion mass, that is, $h\nu = m_A\, c^2\, [1 + O(\beta^2)/2]$, where $\beta \approx 10^{-3}$ is the galactic virial velocity, and h is the Planck constant. The signal is thus monochromatic to 10^{-6}, and the search for axions is performed by tuning the cavity frequency in small overlapping steps. The time integration at each scanned frequency is one of the limiting factors, which is why the signal-to-noise ratio (SNR) is of prime importance. It can be estimated from the Dicke radiometer equation (16):

$$SNR = \left(P/k_B T_{syst}\right)\left(\Delta t/\Delta\nu\right)^{1/2}, \tag{2}$$

where P is the detection power given by (1), which is of the order of 10^{-23} W or less, k_B is the Boltzmann constant, $T_{syst} = T + T_N$, that is, the sum of the physical temperature T and the intrinsic amplifier noise temperature T_N, Δt is the time integration, and $\Delta\nu$ is the amplifier frequency bandwidth. SNR can be maximized by lowering T_{syst}, which means reaching a low temperature for the cavity and working close to the quantum limit for the first amplifier.

The main figures of merit for the haloscope that can be deduced from Eqs 1 and 2 are B^2V and T_{syst}, which require development of high-field magnets and operation at ultra-low temperature, that is, down to a few tens of mK. Combined with the use of a high-quality microwave cavity with Q reaching up to 10^6 and an ultra-low-noise amplifier working possibly at the quantum limit, the axion haloscope constitutes the most promising method for axion dark matter searches in the microwave region.

Several haloscopes in operation worldwide focus on different mass regions [17, 18], namely, ADMX, CAPP, CAST/IAXO-RADES, HAYSTAK, GrAHal, ORGAN, and QUAX-aγ. In addition, challenging projects for a plasma haloscope (ALPHA consortium) and a dielectric one (MADMAX) are in preparation, but none of them are ready to probe the 1–3 μeV axion mass range down to the DFSZ sensitivity.

3 Design of the GrAHal-CAPP haloscope

3.1 Large-bore superconducting magnet—the "outsert" part of the modular Grenoble hybrid magnet

The Grenoble Axion Haloscope project (GrAHal) [19] is based on the use of the modular hybrid magnet platform of LNCMI-Grenoble combining resistive insert magnets requiring 2×12MW of electrical power with a large-bore superconducting "outsert" to reach a total magnetic field of 43 T in a first step [20]. The utilities to operate such a hybrid magnet comprise a fully dedicated cryoplant producing up to 140 L/h of LHe, a cryogenic satellite providing the pressurized superfluid He needed to cool the magnet to 1.8 K, control and safety systems including a dump resistor to extract the 85 MJ of stored energy in case of a magnet quench, and a dedicated 7500 A/±15 V power converter. These items are in addition to the 24-MW electrical power plant for resistive magnets that include water cooling circuits. Ongoing upgrades of the electrical power plant to 30 MW will allow reaching a magnetic field of approximately 46 T, surpassing the highest DC magnetic field ever produced worldwide.

One of the specifics of the Grenoble hybrid magnet is its modularity, allowing various magnetic field configurations ranging from 9 T in the 810-mm diameter (Figure 1) to 43 T in the 34-mm diameter by adding the resistive inserts [20]. Based on Sikivie's haloscope principle, all these field configurations can be equipped by RF cavities of different diameters and, therefore, various resonant frequencies for axion/ALPs dark matter search, and this offers the unique opportunity to cover, in principle, the entire axion mass range from 1 to 300 μeV [19].

The commissioning of the large-bore superconducting coil was successfully achieved in July 2023 up to 8.5 T in a first step [21] and is being pursued in the hybrid magnet configurations. The GrAHal-CAPP haloscope will use the 9 T/810-mm diameter magnetic field configuration of the Grenoble hybrid magnet platform, offering the unpreceded figure of merit $B^2V \approx 34.5$ T^{2}m^3 for the 1–3 μeV axion/ALPs mass range.

3.2 Light Cu RF cavity development with the frequency tuning mechanism

A light Cu RF cavity will be built at CAPP from a high-purity OFHC Cu sheet of 0.5 mm wrapped to obtain a cylinder and laser-welded to achieve high-quality bounding contact (Figure 2). The top and bottom plates of the cavity will be made from an Al layer with 0.5 mm of OFHC Cu. The lowest targeted resonant frequency will be approximately 328 MHz, corresponding to an internal diameter of 700 mm for a height of 1,400 mm and a total volume of 538 L. The total weight of the cavity will be around 25 kg for 0.5 mm of Cu sidewall thickness.

As the cavity size increases, the tuning rods also grow in size and weight, posing challenges in cryogenic conditions. Two critical considerations emerge: first, generating sufficient mechanical support force without burdening the cooling efficiency of the refrigerator and second, ensuring efficient cooling of the tuning rods along with the cavity without losing the cavity Q factor. CAPP
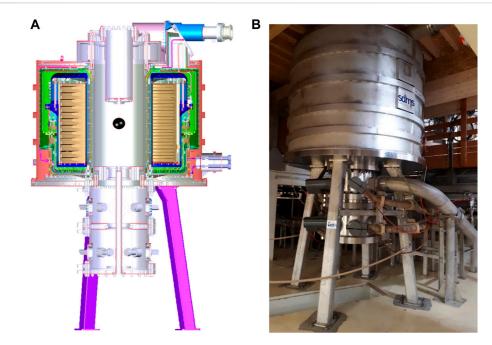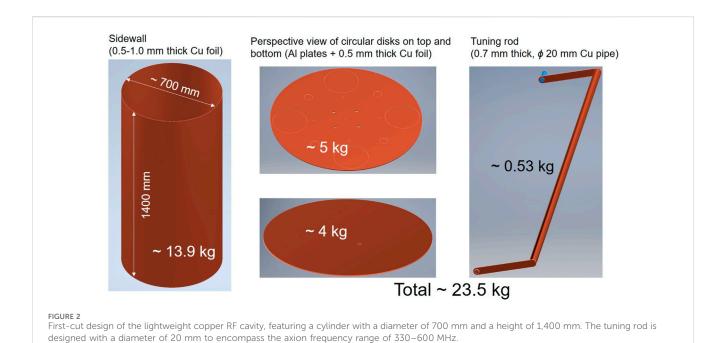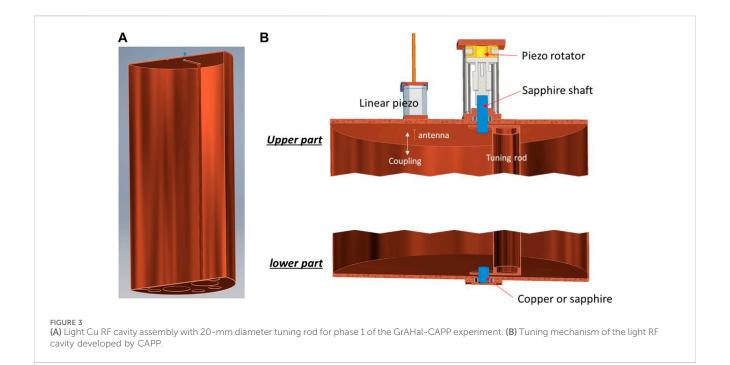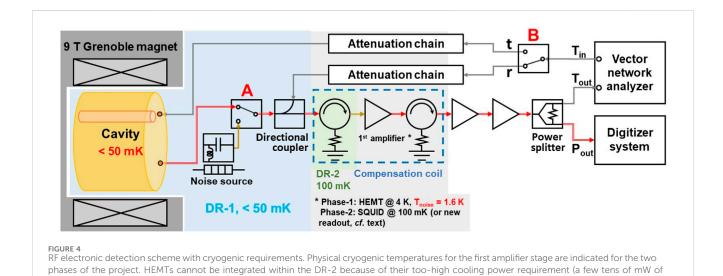
FIGURE 1
(A) Cut view of the cryostat and large-bore superconducting outsert of the Grenoble hybrid magnet. **(B)** Magnet as built in operation at LNCMI-Grenoble. The total height is approximately 5.4 m for a total weight of approximately 52 tons. Mechanical structures above and below the magnet aperture are water-cooling boxes for the 24-MW resistive inserts used to reach higher magnetic fields. They will not be used for the GrAHal-CAPP haloscope described in this article.

FIGURE 2
First-cut design of the lightweight copper RF cavity, featuring a cylinder with a diameter of 700 mm and a height of 1,400 mm. The tuning rod is designed with a diameter of 20 mm to encompass the axion frequency range of 330–600 MHz.

addresses both these challenges by crafting the massive tuning rods from thin copper foil, minimizing the required support force and utilizing sapphire as a mediator to maintain contact between the tuning rods and the cavity's outer space, ensuring cooling without generating transmission modes and thus energy loss from inside the cavity. The movement of the tuning rods is controlled using a piezoelectric rotator with gears, enabling precise motion with sub-millidegree accuracy. The size, position, and number of tuning rods are adjustable to scan the frequency range of 330–600 MHz comprehensively. Further extending the frequency range to 200 MHz by replacing the copper tuning rod with sapphire is also being studied.

FIGURE 3
(A) Light Cu RF cavity assembly with 20-mm diameter tuning rod for phase 1 of the GrAHal-CAPP experiment. **(B)** Tuning mechanism of the light RF cavity developed by CAPP.

FIGURE 4
RF electronic detection scheme with cryogenic requirements. Physical cryogenic temperatures for the first amplifier stage are indicated for the two phases of the project. HEMTs cannot be integrated within the DR-2 because of their too-high cooling power requirement (a few tens of mW of dissipation). Noise temperatures are 1.6 K for phase 1, and the target for phase 2 is 100 mK. A second amplification stage (HEMT @ 4K) is not represented for simplicity.

The lightweight RF cavity (Figure 2), as well as the frequency tuning mechanism (Figure 3), are similar to the ones developed and used by CAPP to reach the DFSZ limit for axion search in the mass range approximately 4.55 μeV [22]. For this experiment, a high Q factor exceeding 10^5 was reached, and the cavity was successfully cooled to 25 mK.

3.3 RF measuring chain

The RF receiver chain is carefully designed to minimize noise. As shown in Figure 4, power from the cavity goes through a directional coupler and two circulators, one per each side of a first cryogenic HEMT (high electron mobility transistor) amplifier with a noise temperature of 1.6 K and a gain of approximately 30 dB for the targeted frequency range 200–600 MHz. The antenna to pick up the signal from the cavity will be made of copper to minimize attenuation, and the rest of the connection to the first amplifier will be through Nb-Ti superconducting cables with a typical attenuation of less than 0.5 dB per meter. The cryogenic switch will be used to make accurate *in situ* noise temperature measurements.

Temperature requirements for the RF cavity and the first RF amplification stage have driven the design of the haloscope cryostat and cooling systems described in the next paragraph, which will also take into account phase 2 of the project using SQUID for the first amplification stage instead of HEMT.
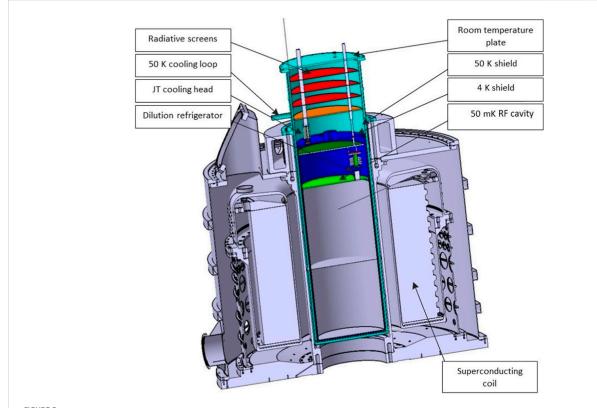
FIGURE 5
Schematic integration of the haloscope cryostat within the large-bore superconducting magnet. The RF cavity at 50 mK is shown in light green with its connection to the first dilution refrigerator. The plate in dark green is at 1 K. The thermal shield in blue will be approximately 4 K; it is embedded in the 50-K shield shown in orange. Three radiative screens will cover the 50-K shield. The tube on the left side, for He flow, is closed by a powerful Joule Thomson (JT) valve to cool the 4-K shield.

A field compensation coil is needed for phase 1, mostly for the circulators operating in a background magnetic field up to 1.5 T (Figure 4), as well as for SQUID in phase 2. HEMT amplifiers are known to not be sensitive to magnetic fields when they are oriented parallel to magnetic field lines [23]. This has been confirmed by recent measurements of the gain and noise of a low-noise factory HEMT amplifier performed at Institut Néel up to 12 T.

3.4 Haloscope cryogenics with the superconducting compensation coil

3.4.1 Cryogenics

A specific cryostat must be built for the 700-mm diameter RF cavity that will be cooled to a temperature below 50 mK with a 3He/4He dilution refrigerator (DR) able to extract 300 μW at 100 mK. The volume optimization of the cryostat is ongoing with three, or possibly two, thermal shields for the selected intermediate temperature stages of 50 K and 4 K (Figure 5). The proposed cryogenic scheme uses the electronics as an additional DR stage to reach 100 mK and extract 50 μW at this temperature, that is, a double-DR configuration. This is an original architecture that could also be applied to other projects requiring several cold stages in distant locations, such as several quantum processors for quantum computing. The required cooling performances of the overall cryogenics are similar to the DR system used in astrophysical

applications developed at Institut Néel for the NIKA [24] and CONCERTO [25] experiments. The choice of the "dry" cryogenic approach, avoiding the use of cryogenic liquids, relies on a 4-K powerful pulse-tube cryocooler. All equipment sensitive to the stray magnetic field will be deported to approximately 4.5 m from the magnet center, that is, in a field region with B ≤ 10 mT.

To limit the transmission of mechanical vibrations, the cryocooler and the pumping system will be installed in a separate box and coupled to the experimental cryostat by a flexible cryogenic line of several meters. The thermal coupling of the cryostat with the two stages of the cryocooler is realized with a pressurized helium loop, which is developed by Absolut System and tested at the Néel Institute for applications to quantum computing (QuCUBE project [26]).

3.4.2 Superconducting compensation coil

The magnetic field profile of the large bore superconducting "outsert" coil was computed for a 9-T central field (Figure 6). Within the cavity volume of 0.538 m^3, the average B_z component is equal to 7.993 T while the Root Mean Square of B_z is equal to 8.055 T. To reduce the magnetic stray field at the level of the first RF circulator (Figure 4), a field cancelation coil will be built and integrated at 1,544 mm from the magnetic field center. Several coil design options are being considered to provide a magnetic compensation field up to 2 T, either a commercial Nb-Ti coil or one based on a high-temperature superconductor (HTS). The parameters of the pre-designed compensation coil used for the field computation given in Figure 6 are summarized in Table 1.
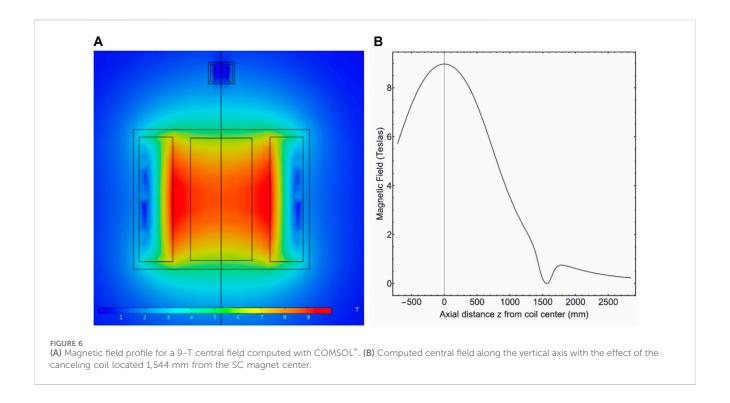
FIGURE 6
(A) Magnetic field profile for a 9-T central field computed with COMSOL®. **(B)** Computed central field along the vertical axis with the effect of the canceling coil located 1,544 mm from the SC magnet center.

TABLE 1 Main parameters of the field compensation coil.

Coil inner radius (mm)	Coil outer radius (mm)	Coil height (mm)	Engineering current density (nominal)
75	125	200	29 A/mm^2

Robust current leads (CL) must also be designed and built to power the compensation coil. For conduction-cooled CL, the minimal heat inleak is approximately 2×50 mW/A on the 4-K shield of the cryostat (Figure 5), which is too high for the cryogenic budget. To cope with this problem, heat sinking made by a heat exchanger cooled by He Gaz will be added to the 50-K shield. A detailed study is ongoing to determine if the cold part of the CL will be based on the HTS.

For the 9-T central field, the axial ascending magnetic force that will be exerted on the compensation coil and transmitted to the 4-K shield of the cryostat is estimated to be approximately 2.5 tons. For 2 mm off-centering of both coils, the "runaway" radial force will be equal to 140 kg, and the resulting magnetic torque will be approximately 21 kg m. With every 1 degree of misalignment, an additional magnetic torque of 17 kg m will be added or subtracted.

4 Targeted sensitivities

4.1 GrAHal-CAPP phase 1 using HEMT amplifiers and field compensation coil

The targeted sensitivity for phase 1 is given in Figure 7. It is obtained from Equations 1, 2 and the input parameters summarized in Table 2. The main result obtained from a conservative approach gives a scan rate on the order of 0.5 MHz/day at the DFSZ sensitivity, meaning that the range 330–600 MHz can be covered in less than 2 years.

4.2 GrAHal-CAPP phase 2 using a quantum amplifier

For the 300–600 MHz range, SQUIDs are the optimum linear quantum amplifier choice for the first stage of the receiver chain. A dedicated R&D program at CAPP aims to reduce the total system noise to below 100 mK using new RF-readout techniques [27]. This new detection scheme will be implemented inside the DR-2 (Figure 4) once its proper functioning is fully validated at CAPP, which could occur before the end of the data taking of phase 1.

5 Conclusion and perspectives

A new haloscope is proposed by the GrAHal-CAPP collaboration based on the use of the superconducting "outsert" coil of the Grenoble hybrid magnet, providing an unpreceded figure of merit for this type of experiment, that is, $B^2V \approx 34.5$ T^{2}m^3. During phase 1, it will allow a significant extension of the state-of-the-art exclusion limit for the 1–3 μeV axion/ALPs mass range by reaching the DFSZ limit with less than a 2-year integration time. Phase 2 of this experiment targets replacing the HEMT amplifier with a low-noise SQUID amplifier to gain an additional factor of about three on the axion DM search sensitivity. In other words, the axion–diphoton coupling constant $g_{A\gamma\gamma}$ will reach the limit at the bottom of the yellow band in Figure 7.
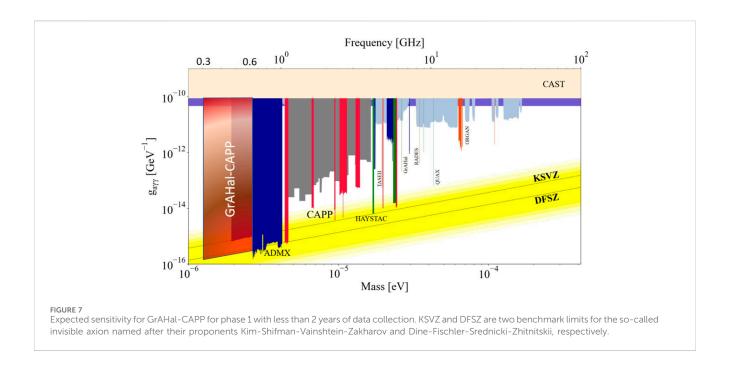
FIGURE 7
Expected sensitivity for GrAHal-CAPP for phase 1 with less than 2 years of data collection. KSVZ and DFSZ are two benchmark limits for the so-called invisible axion named after their proponents Kim-Shifman-Vainshtein-Zakharov and Dine-Fischler-Srednicki-Zhitnitskii, respectively.

TABLE 2 Main input parameters used to estimate the exclusion limits given in Figure 7.

$\langle B^2 V \rangle$ at 9 T central field	Q at 4.4 K	C_{010}	Noise T (K)	$g_{A\gamma\gamma}$
34.4 T^2 m^3	1–$2\ 10^5$	0.63–0.69	1.6	DFSZ

Data availability statement

The raw data supporting the conclusions of this article will be made available by the authors, without undue reservation.

Author contributions

PPu: writing–original draft and writing–review and editing. PC: writing–original draft and writing–review and editing. OK: writing–original draft and writing–review and editing. RB: writing–original draft and writing–review and editing. CB: writing–original draft and writing–review and editing. HB: writing–original draft and writing–review and editing. WC: writing–original draft and writing–review and editing. TG: writing–original draft and writing–review and editing. PPe: writing–original draft and writing–review and editing. YS: writing–original draft and writing–review and editing. AT: writing–original draft and writing–review and editing. JV: writing–original draft and writing–review and editing.

Funding

Acknowledgments

Conflict of interest

The authors declare that the research was conducted in the absence of any commercial or financial relationships that could be construed as a potential conflict of interest.

Publisher's note

References

1. Weinberg S. A new light boson? *Phys Rev Lett* (1978) 40:223–6. doi:10.1103/PhysRevLett.40.223

2. Wilczek F. Problem of strong P and T invariance in the presence of instantons. *Phys Rev Lett* (1978) 40:279–82. doi:10.1103/PhysRevLett.40.279

3. Peccei R-D, Quinn H-R. CP conservation in the presence of pseudoparticles. *Phys Rev Lett* (1977) 38:1440–3. doi:10.1103/PhysRevLett.38.1440

4. Svrek P, Witten E. Axions in string theory. *High Energ Phys* (2006):06051. doi:10.1088/1126-6708/2006/06/051

5. Kim J-E. Weak-interaction singlet and StrongCPInvariance. *Phys Rev Lett* (1979) 43:103–7. doi:10.1103/physrevlett.43.103

6. Cicoli M, Goodsell M, Ringwald A. The type IIB string axiverse and its low-energy phenomenology. *J High Energ Phys*. (2012) 2012(10):146. doi:10.1007/jhep10(2012)146

7. Abbott L-F, Sikivie P. A cosmological bound on the invisible axion. *Phys.Lett.* (1983) B120:133–6. doi:10.1016/0370-2693(83)90638-x

8. Bradlay R, Clarke J, Kinion D, Rosenberg LJ, van Bibber K, Matsuki S, et al. Microwave cavity searches for dark-matter axions. *Rev Mod Phys* (2003) 75:777–817. doi:10.1103/revmodphys.75.777

9. Arias P, Cadamuro D, Goodsell M, Jaeckel J, Redondo J, Ringwald A. WISPy cold dark matter. *J Cosmol Astropart Phys* (2012) 06:013. doi:10.1088/1475-7516/2012/06/013

10. Ringwald A. Exploring the role of axions and other WISPs in the dark universe. *Dark Universe* (2012) 1:116–35. doi:10.1016/j.dark.2012.10.008

11. Workman RL, Burkert VD, Crede V, Klempt E, Thoma U, Tiator L, et al. Particle Data Group. *Prog Theor Exp Phys 2022* (2022) 083C01:1038–1055. Available at: https://pdg.lbl.gov/ (Accessed March 25, 2024). doi:10.1093/ptep/ptac097

12. Meyer M, Horns D, Raue M. First lower limits on the photon-axion-like particle coupling from very high energy gamma-ray observations. *Phys Rev D* (2013) 87:035027. doi:10.1103/physrevd.87.035027

13. Miller Bertolami M-M, Melendez B, Althaus L, Isern J. Revisiting the axion bounds from the Galactic white dwarf luminosity function. *JCAP* (2014) 10:069. doi:10.1088/1475-7516/2014/10/069

14. Cicoli M, Conlon J-P, Marsh M-C-D, Rummel M. 3.55 keV photon line and its morphology from a 3.55 keV axionlike particle line. *Phys Rev D* (2014) 90:023540. doi:10.1103/physrevd.90.023540

15. Semertzidis Y-K, Youn S. Axion dark matter: how to see it? *Sci Adv* (2022) 8(8): eabm9928. doi:10.1126/sciadv.abm9928

16. Sikivie P. Detection rates for "invisible"-axion searches. *Phys Rev D* (1985) 32:2988–91. doi:10.1103/physrevd.32.2988

17. Dicke R-H. The measurement of thermal radiation at microwave frequencies. *Rev Sci Inst* (1946) 17:268–75. doi:10.1063/1.1770483

18. Sikivie P. Invisible axion search methods. *Rev Mod Phys* (2021) 93:015004. doi:10.1103/revmodphys.93.015004

19. Grenet T, Ballou R, Basto Q, Martineau K, Perrier P, Pugnat P, et al. (2021). *The Grenoble Axion Haloscope platform (GrAHal): development plan and first results.* Available at: https://arxiv.org/abs/2110.14406 (Accessed March 25, 2024).

20. Pugnat P, Barbier R, Berriaud C, Berthier R, Boujet T, Graffin P, et al. 43+T Grenoble hybrid magnet: from final assembly to commissioning of the superconducting outsert. *IEEE Trans Appl Supercond* (2022) 32(6):1–7. doi:10.1109/TASC.2022.3151838

21. Pugnat P, Barbier R, Berriaud C, Debray F, Grandclément C, Hervieu B, et al. Commissioning tests of the 43+T Grenoble hybrid magnet. *IEEE Trans Appl Supercond* (2023) 34:1–5. Accepted for publication in. doi:10.1109/tasc.2023.3341864

22. Yi Andrew K, Ahn S, Kutlu Ç, Kim J, Ko BR, Ivanov BI, et al. Axion dark matter search around 4.55 μeV with dine-fischler-srednicki-zhitnitskii sensitivity. *Phys Rev Lett* (2023) 130:071002. doi:10.1103/physrevlett.130.071002

23. Rodrigues IH, Niepce D, Pourkabirian A, Moschetti G, Schleeh J, Bauch T, et al. On the angular dependence of InP high electron mobility transistors for cryogenic low noise amplifiers in a magnetic field. *AIP Adv* (2019) 9:085004. doi:10.1063/1.5107493

24. Monfardini A, Adam R, Adane A, Ade P, André P, Beelen A, et al. Latest NIKA results and the NIKA-2 project. *J Low Temperature Phys* (2014) 176:787–95. doi:10.1007/s10909-013-0985-4

25. Béthermin M, Gkogkou A, Van Cuyck M, Lagache G, Beelen A, Aravena M, et al. CONCERTO: high-fidelity simulation of millimeter line emissions of galaxies and [CII] intensity mapping. *A&A* (2022) 667:A156. doi:10.1051/0004-6361/202243888

26. de Franceschi S, Meunier T, et Vinet M. *3D integration technology for silicon spin qubits - building a quantum computer with 100 qubits*. Available at: https://cordis.europa.eu/project/id/810504 (Accessed March 25, 2024).

27. Omarov Z, Jeong J, Semertzidis Y-K. Speeding axion haloscope experiments using heterodyne-variance-based detection with a power meter. *Phys Rev D* (2023) 107:103005. doi:10.1103/PhysRevD.107.103005